The Assimilation of Microwave Imager Radiance data in GRAPES_GFS by 4D-VAR

(Hongyi Xiao, Wei Han, Hao Wang, Jinchang Wang, Guiqing Liu)

- Overview and Dateset
- Quality Control
- Bias Correction
- Observation Error
- Case Experiment
- Batch Experiment
- Future plan
- Reference

This study has been jointly supported by:

- National Natural Science Foundation of China (41675108);
- National Key Research and Development Program (2018YFC1506700);
- Second Tibetan Plateau Scientific Expedition and Research Program (2019QZKK0105);
- National Key R&D Program of China (2019YFC1510400)
- National Natural Science Foundation of China (42075155).

Assimilation of MWI: Overview and Dateset

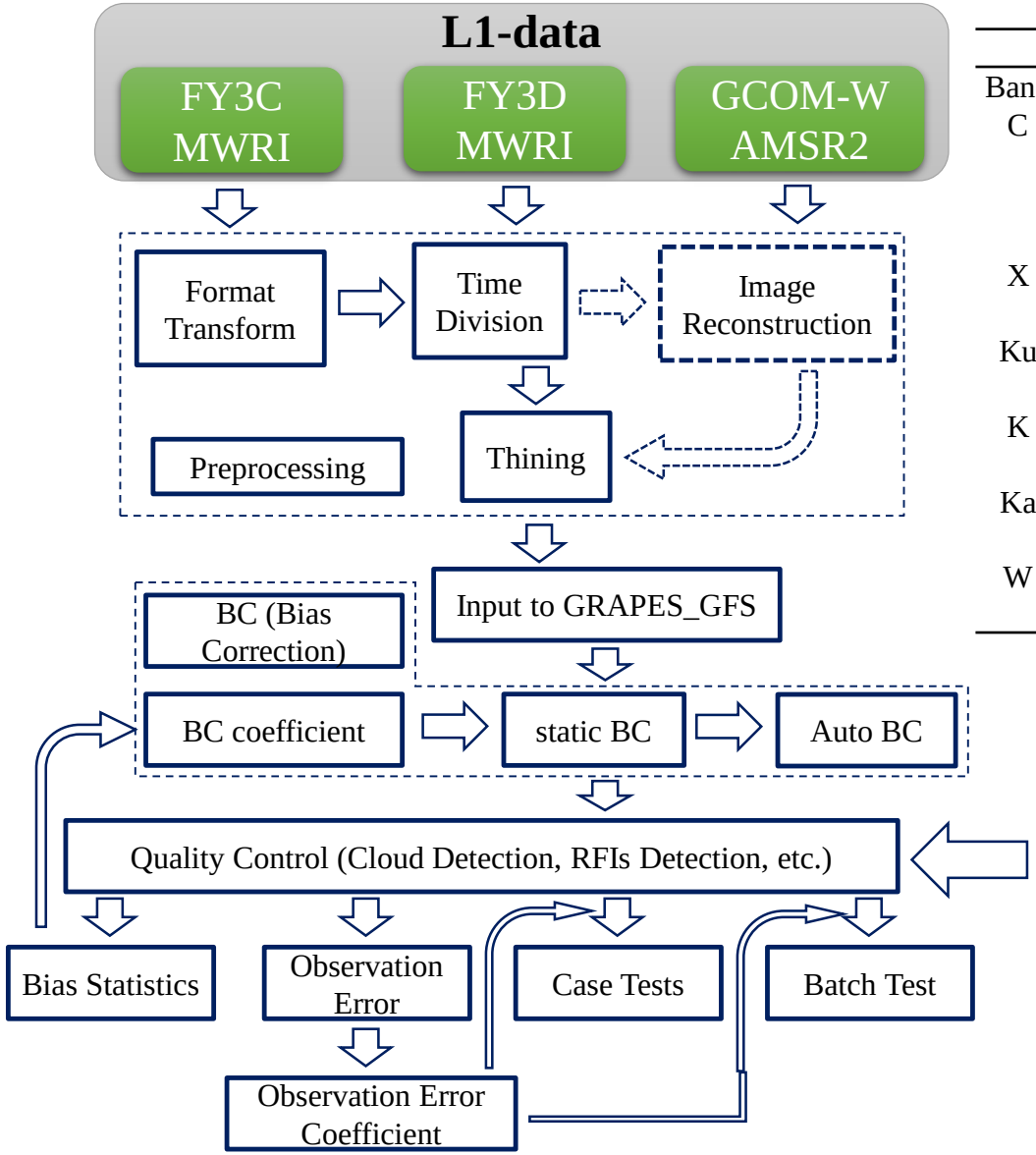

Sensor Name			FY3C/D MWRI		GCOM-W1 AMSR2	
Band	Notation	Polarization	Ch#	Frequency	Ch#	Frequency
C	06V	V			1	6.925
	06H	H			2	6.925
	07V	V			3	7.3
	07H	H			4	7.3
X	10V	V	1	10.65	5	10.65
	10H	H	2	10.65	6	10.65
Ku	19V	V	3	18.7	7	19.35
	19H	H	4	18.7	8	19.35
K	23V	V	5	23.8	9	21.3
	23H	H	6	23.8	10	21.3
Ka	37V	V	7	36.5	11	37
	37H	H	8	36.5	12	37
W	89V	V	9	89.0	13	85.5
	89H	H	10	89.0	14	85.5

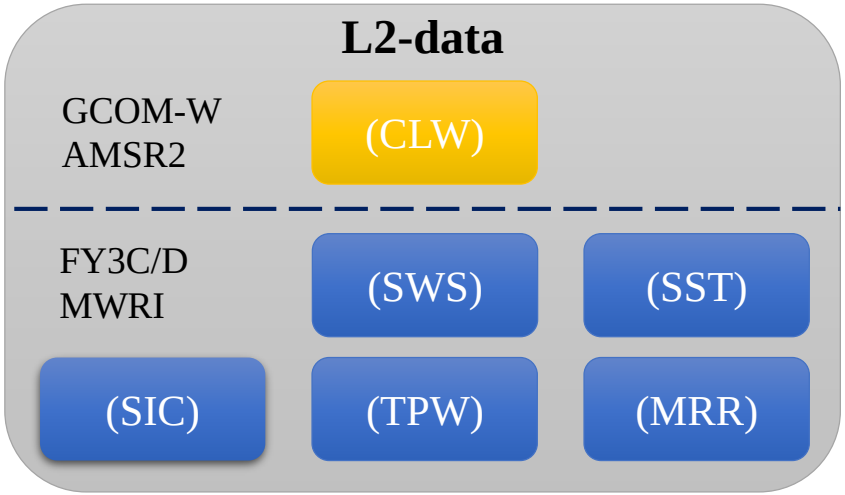

Assimilation of MWI: Quality Control

Factor	QC scheme	Details (the pixels to be screened)	MWRI	AMSR2	Reference
Abnormal	1. Gross value	$70K < T_b < 320K$。	√	√	Huang et al., 2013.
	2. Absolute departure	Absolute departure > 3K。	√	√	Liu et al., 2007; Yang et al., 2016; Yang et al., 2017; Yu et al., 2017; Yu et al., 2018.
	3. Relative departure	Relative departure > $3\sigma_0$。	√	√	Yang et al., 2016.
Surface	4. Surface type	Land/coast/mix surface	√	√	Huang et al., 2013; Liu et al., 2012; Yang et al., 2017; Yu et al., 2017; Yu et al., 2018.
		SIC ≠ 0	√		
		SST < 274K	√		
		Sea ice recognized by ASI algorithm	√	√	Speen et al., 2008; Su et al., 2013.
	5. Land-sea contamination	$T_v^{10} > 175K$ or $T_H^{10} > 95K$。	√		Huang et al., 2013.
	6. Sun-glint	Sun glint angle < 25°(CH1~6)		√	Yang et al., 2017; Yu et al., 2017; Yu et al., 2018.
Weather	6. Abnormal TPW	TPW < 0。	√		Yang et al., 2017.
	7. Abnormal wind speed	SWS > 30m/s。	√		Nielsen-Englyst et al., 2018.
	8. Rain region	MRR ≠ 0	√		Zhu et al., 2016; Liu et al., 2012.
		if anyone is satisfied： $T_V^{37} - 0.979T_H^{37} < 55$; $1.175T_V^{18.7} - 30 > T_V^{37}$; $T_V^{18.7} > 170$; $T_V^{37} > 210$.	√	√	Betthenhausen et al., 2006; Zhao, 2012; Zhao and He, 2013; Guo et al., 2017.
	9. Cloud detection	$T_V^{37} - T_H^{37} < 50$K。	√	√	Connor and Chang, 2000; Krasnopolsky et al., 1995; Dou et al., 2014.
		$\mathrm{CLW(mm)} < \begin{cases} 0.35, & \mathrm{C/X} \\ 0.3, & \mathrm{Ku} \\ 0.25, & \mathrm{K} \\ 0.1, & \mathrm{Ka} \\ 0.02, & \mathrm{W} \end{cases}$	√	√	Kazumori and Liu, 2008.
Anthropic	10.RFIs detection	$T_H^{6.9} - T_H^{7.3} > 0\mathrm{K},\ T_V^{6.9} - T_V^{7.3} > 0\mathrm{K}$		√	Li et al., 2004; Wu and Weng, 2011; Zou et al., 2013b; Feng and Zhao, 2015.
		$T_H^{7.3} - T_H^{10} > 0\mathrm{K},\ T_V^{7.3} - T_V^{10} > 0\mathrm{K}$		√	
		$T_H^{10} - T_H^{19} > 0\mathrm{K},\ T_V^{10} - T_V^{19} > 0\mathrm{K}$	√	√	
		$T_H^{19} - T_H^{23} > 0\mathrm{K},\ T_V^{19} - T_V^{23} > 0\mathrm{K}$	√	√	

Assimilation of MWI: Quality Control

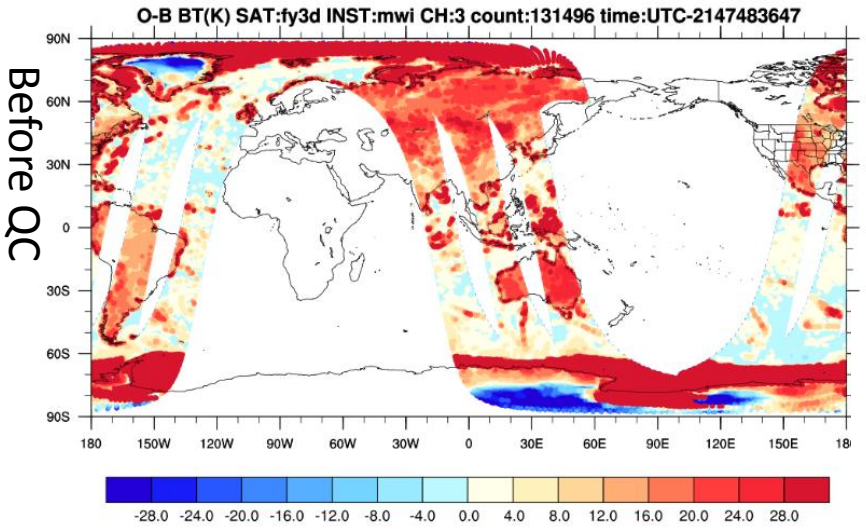

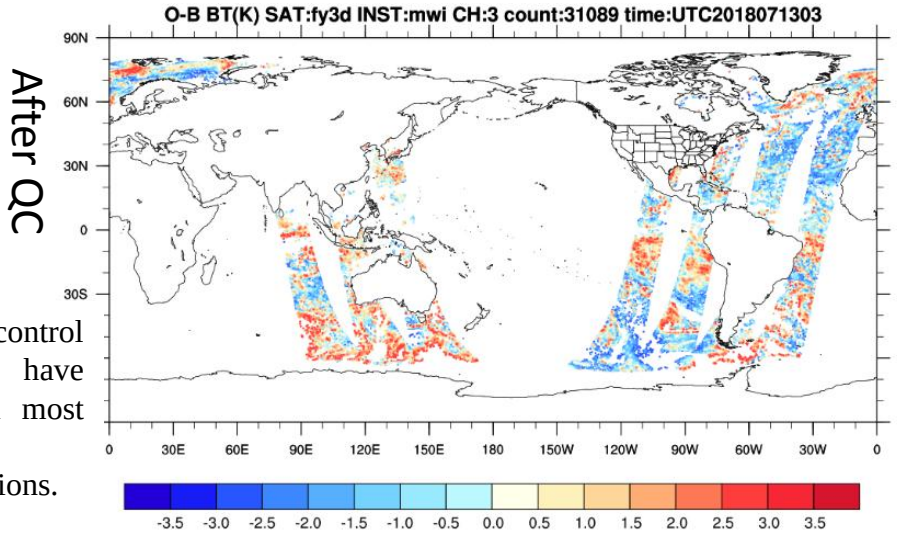

Quality control schemes have screened most invalid observations.

The observation with cloud liquid water path > 0.1. (The algorithm proposed by Grody in 1992 and updated by Zou in 2017 is used to calculated the cloud liquid water.)

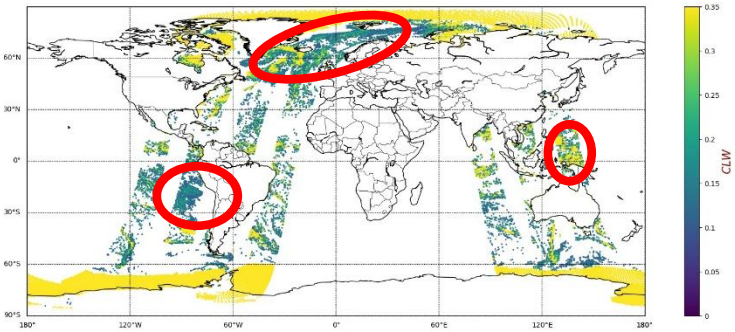

The global cloud map by FY-3D MERSI

July 13th, 2018

Most cloudy regions have been recognized.

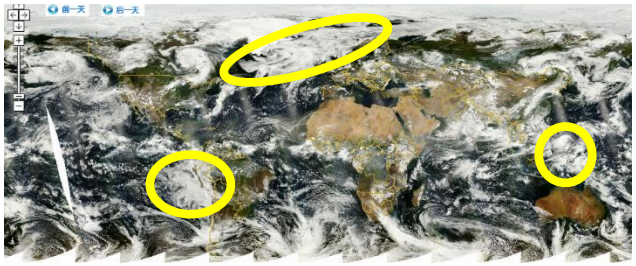

RFI of 19-V channel

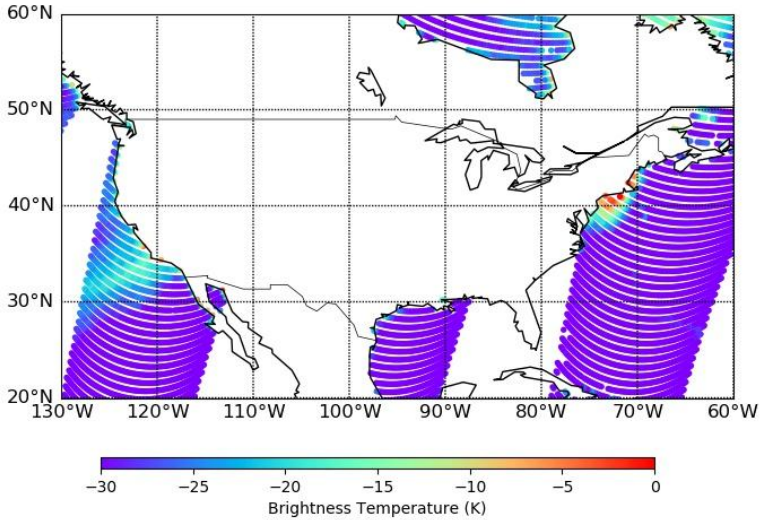

Assimilation of MWI: Quality Control

Sunglint

(© by Wikipedia)

Determination of sunglint angle

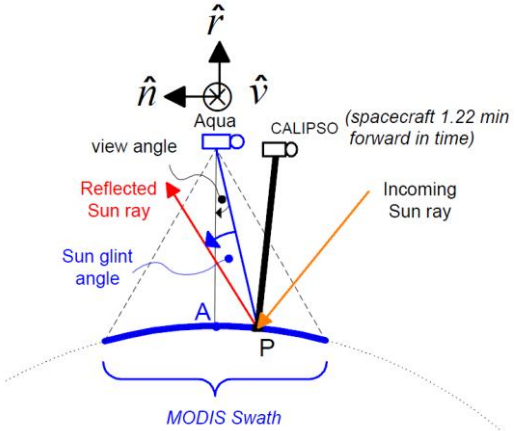

L. M. Mailhe, C. Schiff, J. H. Stadler, 2004: Calipso's mission design: sun-glint avoidance strategies.

AMSR2 sun elevation and sun azimuth

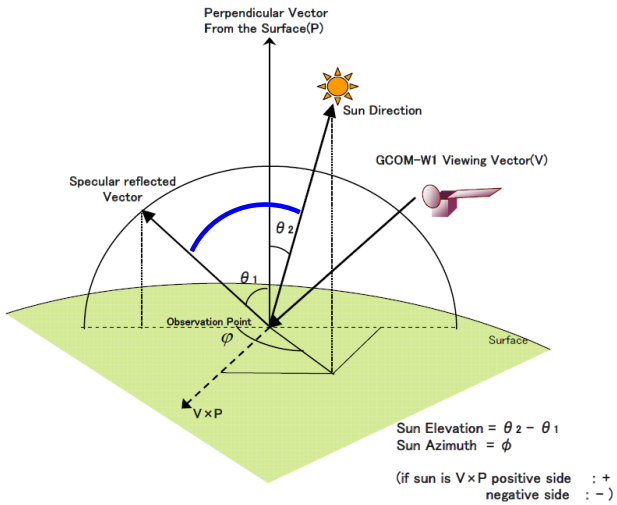

$$\cos\angle COD = \cos\varphi \cdot \sin\theta_1 \cdot \sin\theta_2 + \cos\theta_1 \cdot \cos\theta_2$$

Before sunglint check:

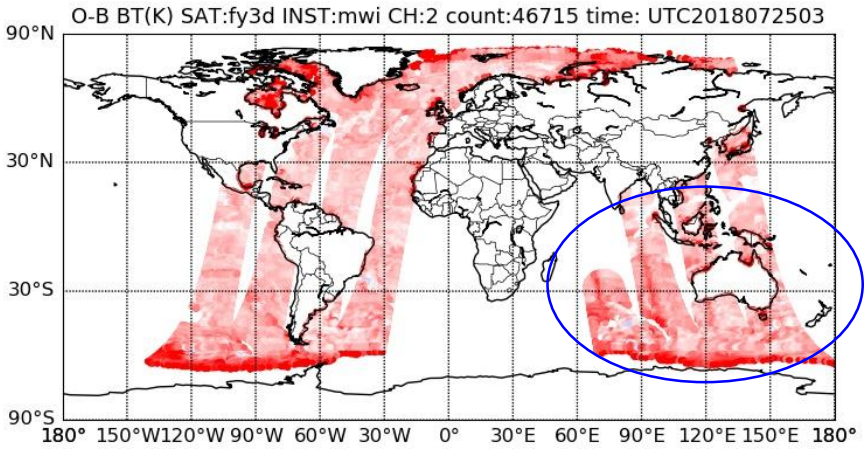

After sunglint check:

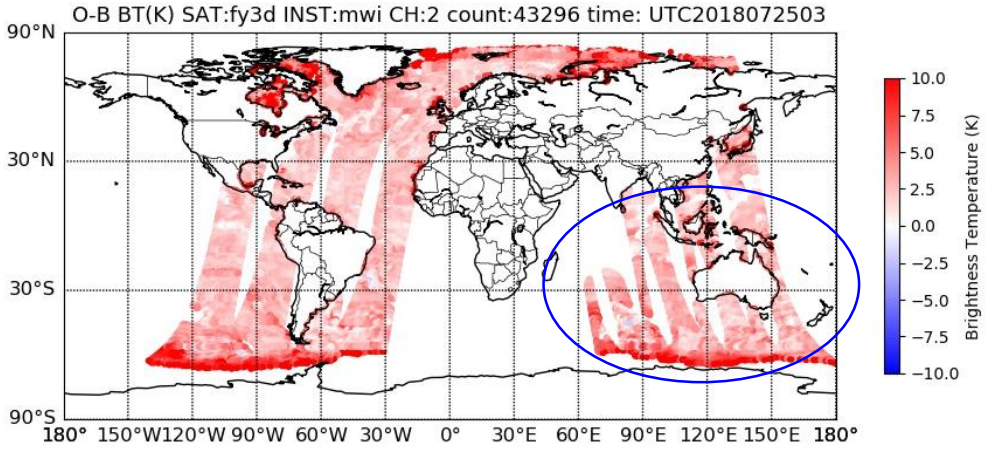

Assimilation of MWI: Quality Control

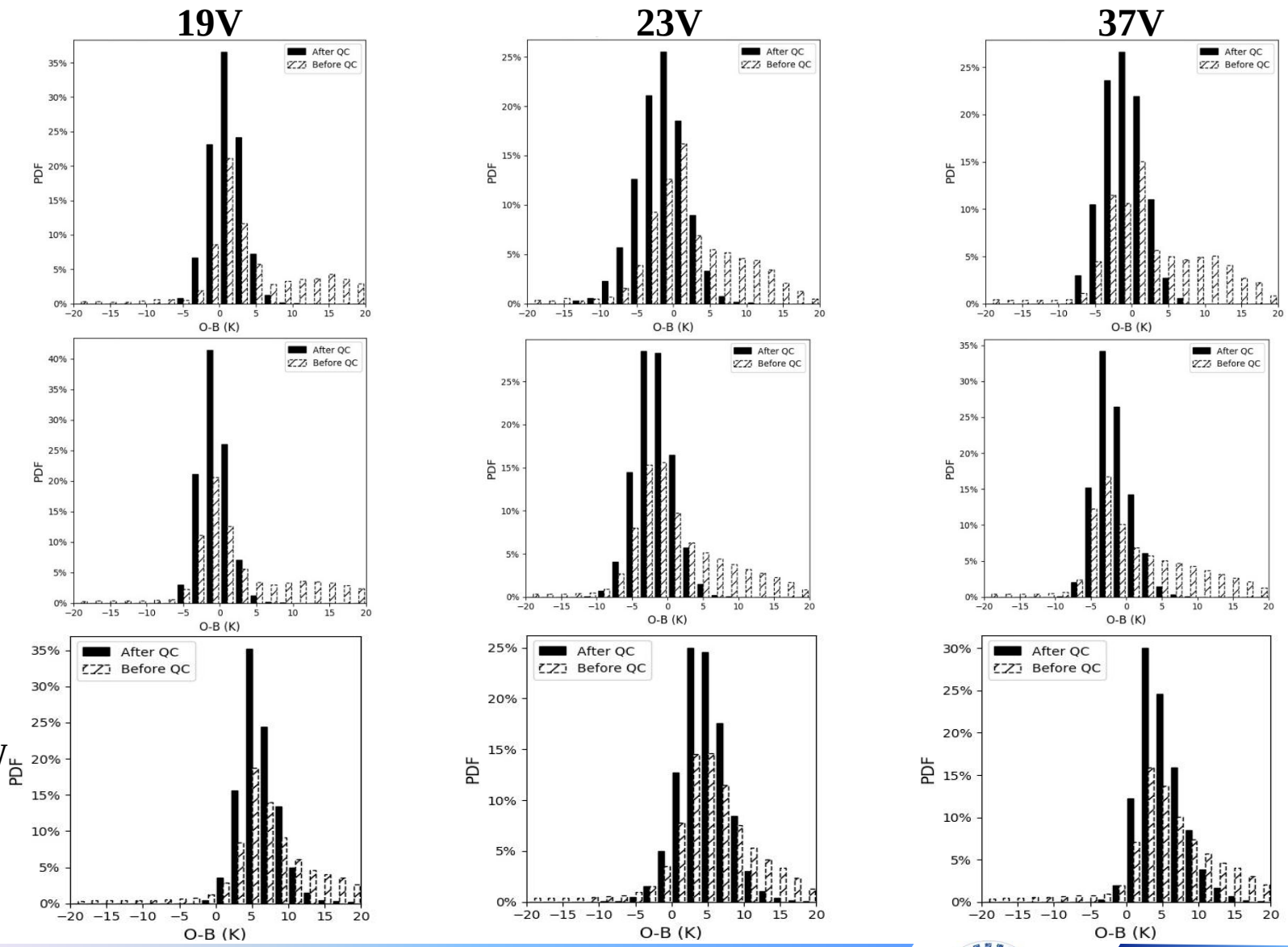

The PDF of O-B is valid after QC.

Assimilation of MWI: Bias Correction

Bias .vs. Channels

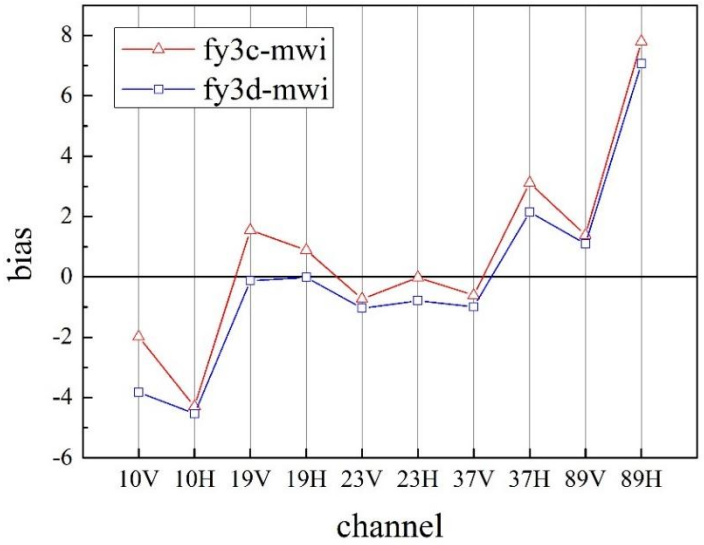

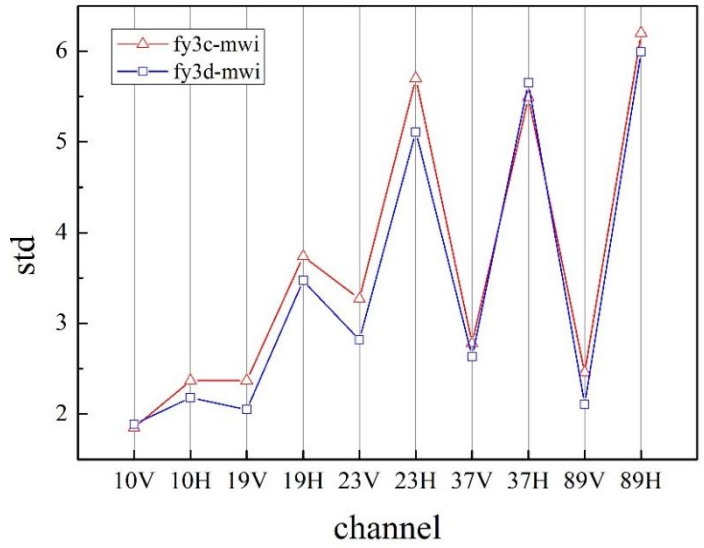

Bias .vs. Scanpos

FY3D MWRI

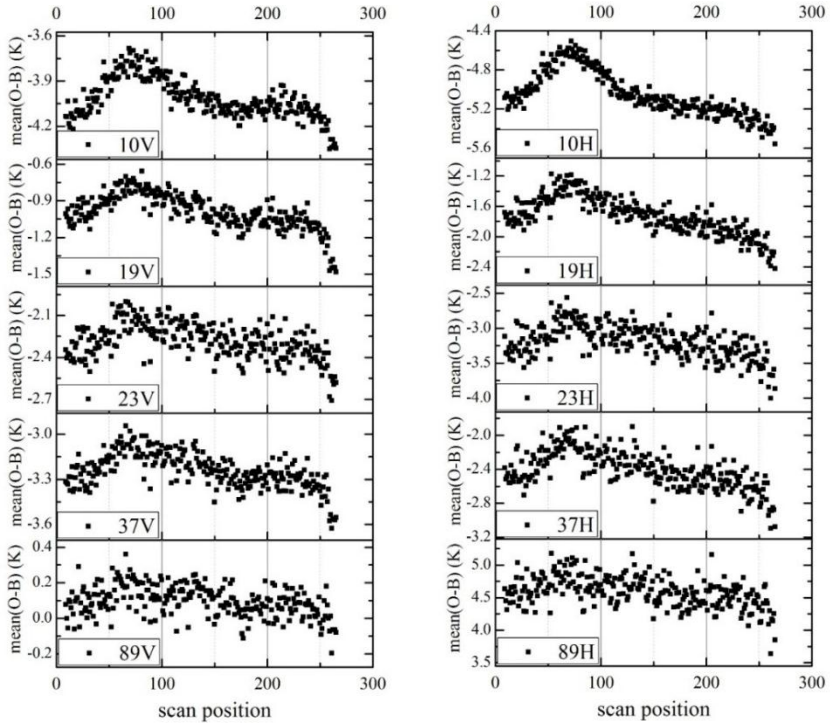

Bias .vs. Ascent/Descent

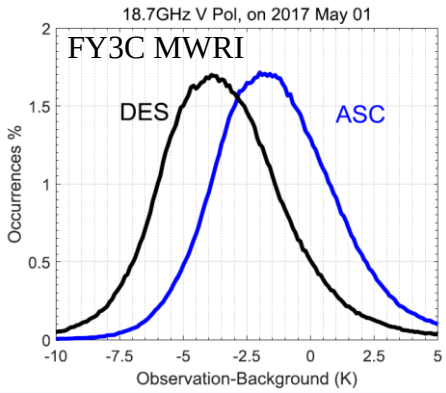

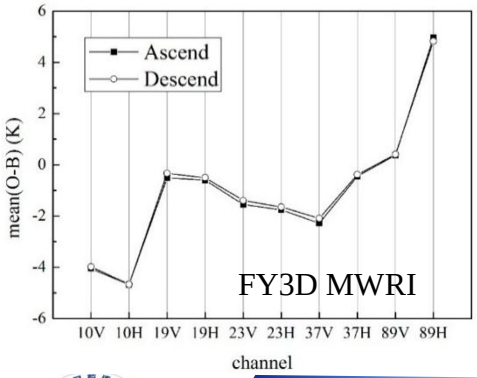

Assimilation of MWI: Bias Correction

scan position

+

1. 1000-300 hPa layer thickness
2. 200-50 hPa layer thickness
3. Surface skin temperature
4. Totalccolumn water vapor

19V **23V** **37V**

FY3C MWRI

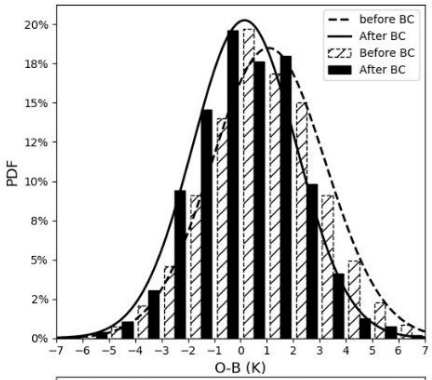

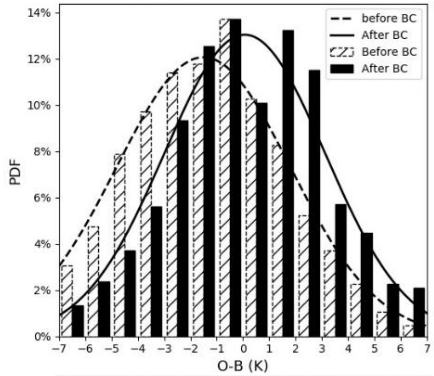

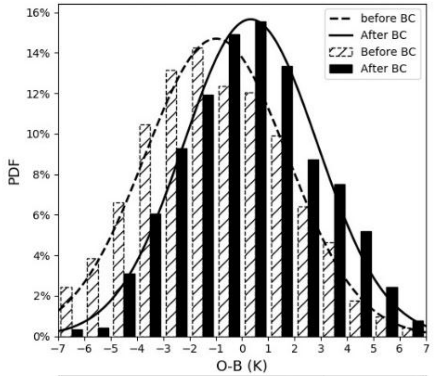

FY3D MWRI

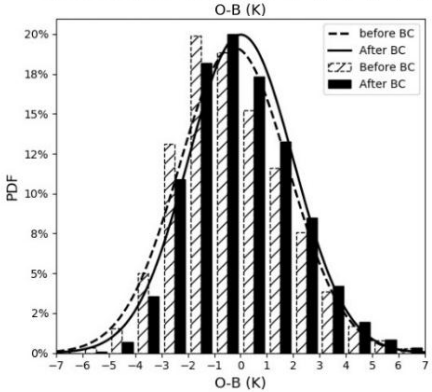

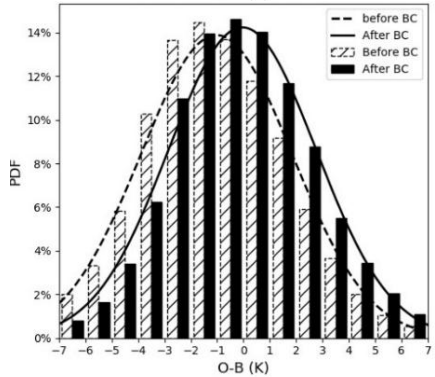

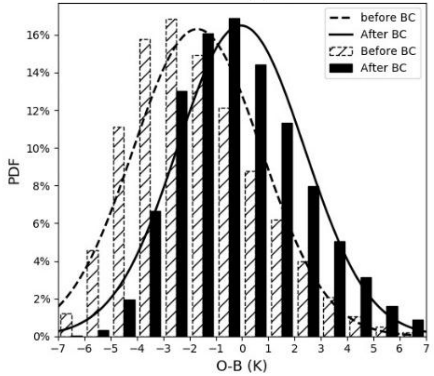

GCOM-W AMSR2

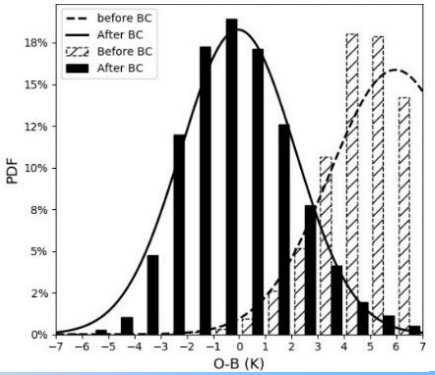

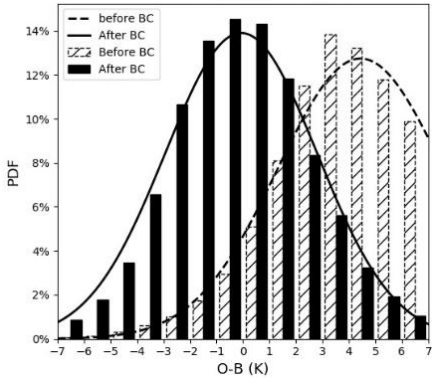

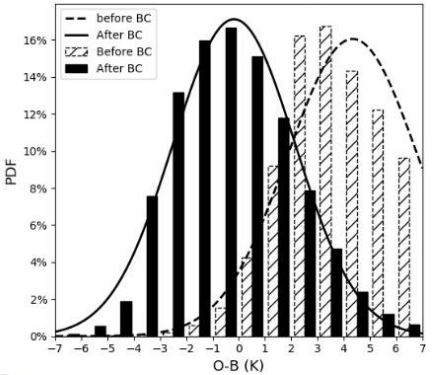

Generally Speaking, the bias correction procedure is effective.

Assimilation of MWI: Observation Error

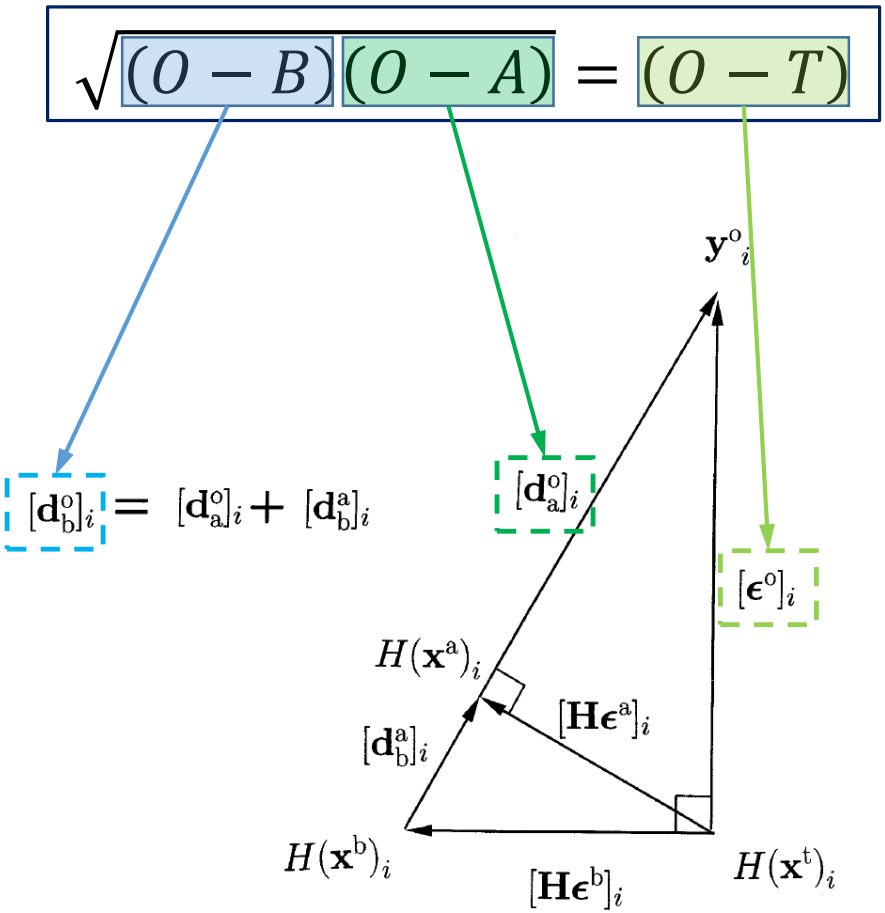

The statistics of observation error of FY3C/D-MWRI and GCOM-W AMSR2 is made by radiances data during 20180713-0725 in GRAPES_GFS。

	FY3C-MWRI	FY3D-MWRI	GCOM-W AMSR2
19V	1.41 K	1.21 K	5.52 K
23V	1.48 K	1.39 K	4.26 K
37V	1.75 K	1.69 K	3.98 K

G. Desroziers, L. Berre, B. Chapnik, et al., 2005: Diagnosis of observation, background and analysis-error statistics in observation space, *Q. J. R. Meteorol. Soc.*, **131**, 3385-3396.

Assimilation of MWI: Case Experiments

Typhoon Shanshan（1813）

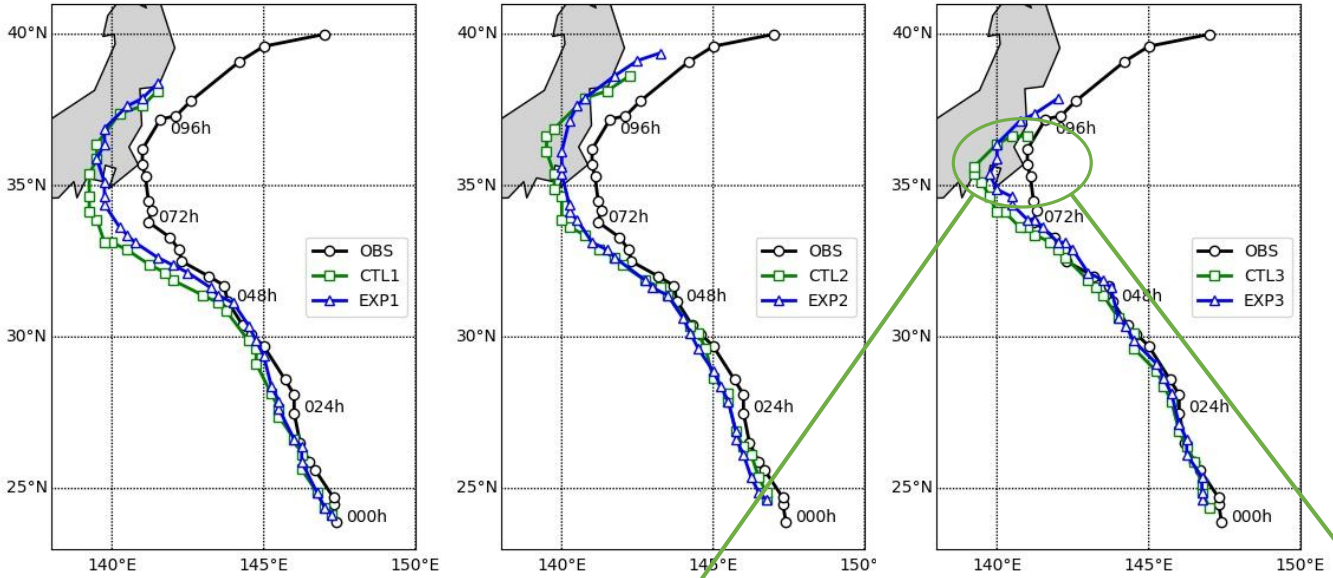

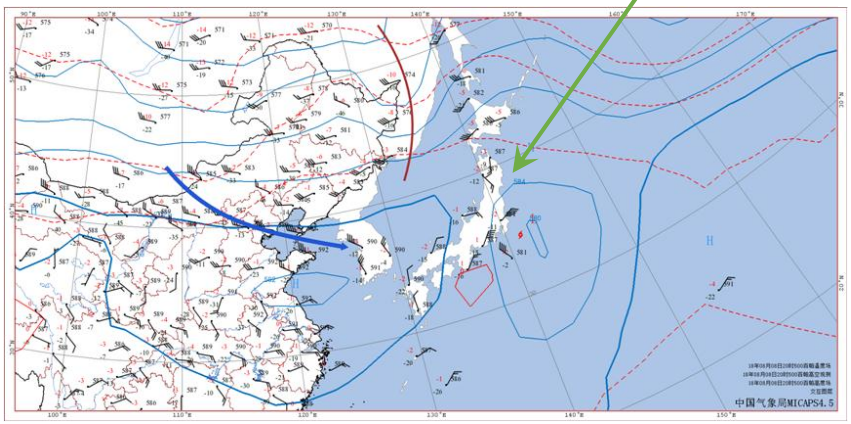

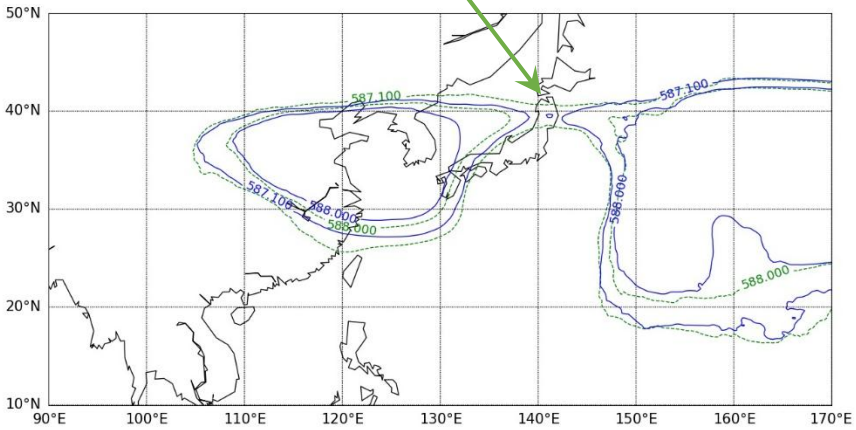

Xiao, H. Y., W. Han*, H. Wang, et al., 2020: Impact of FY-3D MWRI radiance assimilation in GRAPES 4D-Var on Forecasts of Typhoon Shanshan, *J. Meteor. Res.*, **34**(4): 836-850, doi: 10.1007/s13351-020-9122-x.

Assimilation of MWI: Batch Experiments

Version：GRAPES_GFS3.0

CTRL：Default Setting

EXP1：CTL+ orange region

EXP2：EXP1 + blue region

Data Segment：One month（20180725~20180825）

Thinning Scheme：200km

Bias Correction：Statistics by data in 20180713-0725

Sensor Name			FY3C MWRI		FY3D MWRI		GCOM-W1 AMSR2	
Band	Notation	Polarization	Ch#	Frequency	Ch#	Frequency	Ch#	Frequency
C	06V	V					1	6.925
	06H	H					2	6.925
	07V	V					3	7.3
	07H	H					4	7.3
X	10V	V	1	10.65	1	10.65	5	10.65
	10H	H	2	10.65	2	10.65	6	10.65
Ku	19V	V	3	18.7	3	18.7	7	19.35
	19H	H	4	18.7	4	18.7	8	19.35
K	23V	V	5	23.8	5	23.8	9	21.3
	23H	H	6	23.8	6	23.8	10	21.3
Ka	37V	V	7	36.5	7	36.5	11	37
	37H	H	8	36.5	8	36.5	12	37
W	89V	V	9	89.0	9	89.0	13	85.5
	89H	H	10	89.0	10	89.0	14	85.5

Assimilation of MWI: Batch Experiments

EXP1 .vs. CTL

Humidity (>500hPa) is improved。

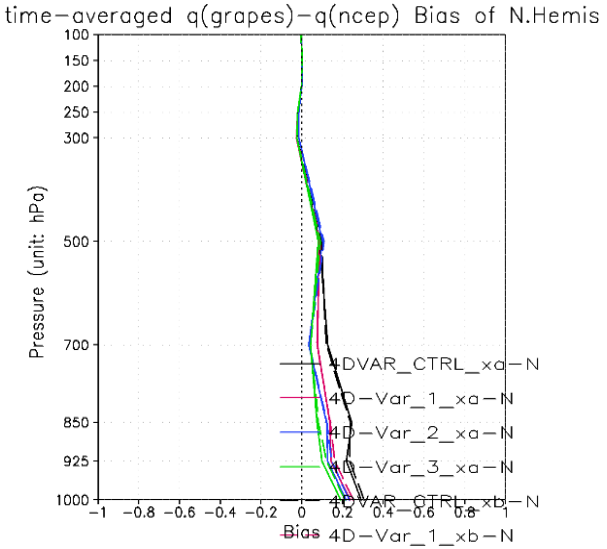

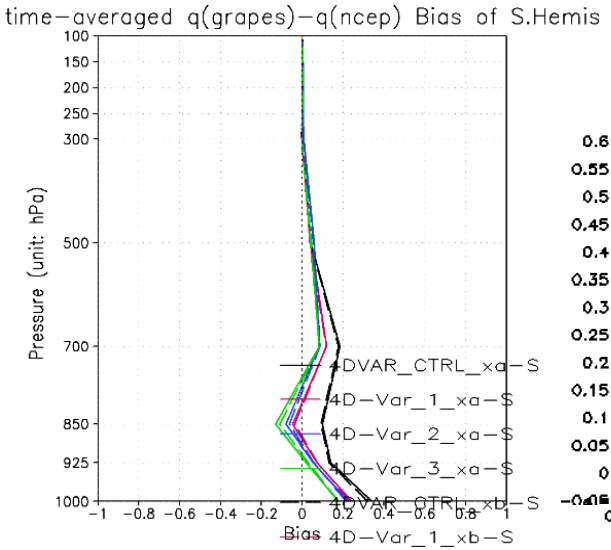

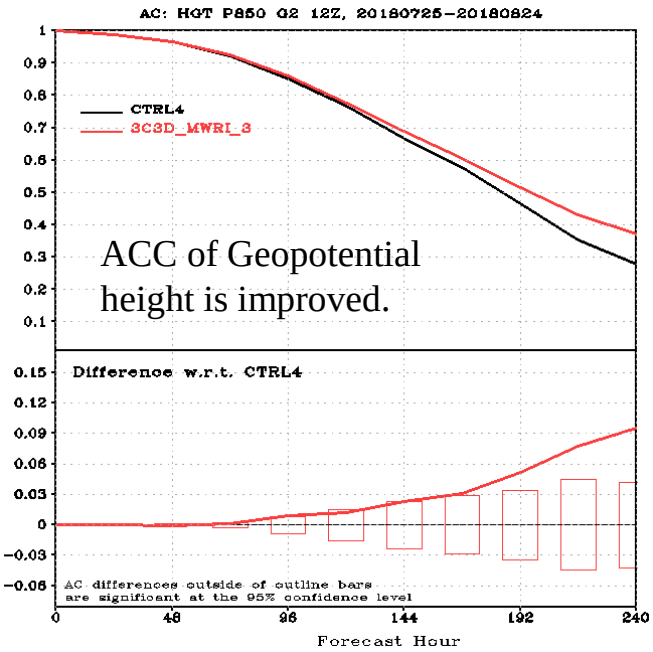

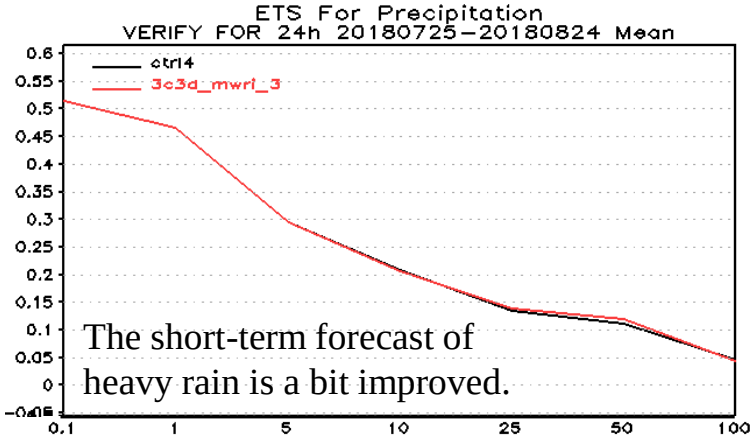

Score Card for 3c3d_mwri_3 against ctrl4

Domain	Parameter	Level	Anomaly Correlation	RMS Error
NH	UWND	250		
		500		
		850		
	VWND	250		
		500		
		850		
	TEMP	250		
		500		
		850		
	HGT	250		
		500		
		700		
SH	UWND	250		
		500		
		850		
	VWND	250		
		500		
		850		
	TEMP	250		
		500		
		850		
	HGT	250		
		500		
		700		
EASI	UWND	250		
		500		
		850		
	VWND	250		
		500		
		850		
	TEMP	250		
		500		
		850		
	HGT	250		
		500		
		700		
TRO	UWND	250		
		500		
		850		
	VWND	250		
		500		
		850		
	TEMP	250		
		500		
		850		
	HGT	250		
		500		
		700		

▲: Far better ▲: Better ▪: Better but not significant ▪: Equality
▼: Far worse ▼: Worse ▪: Worse but not significant

Assimilation of FY3C&D-MWRI has positive effects on forecast in southern hemisphere.

Assimilation of MWI: Batch Experiments

EXP2 .vs. EXP1

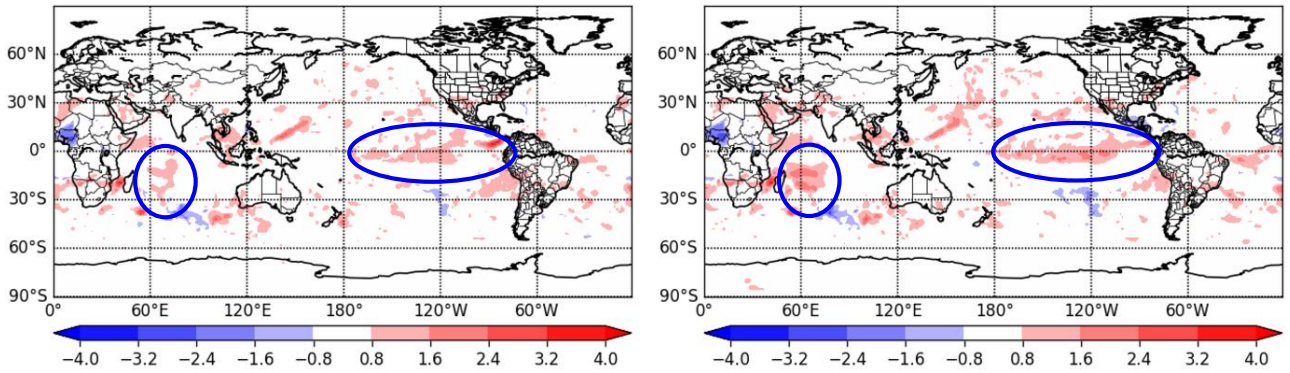

Bias of Humidity field (850hPa 72h) becomes larger after assimilation all the three MWIs.

Grid precipitaion verification

Point precipitation verification

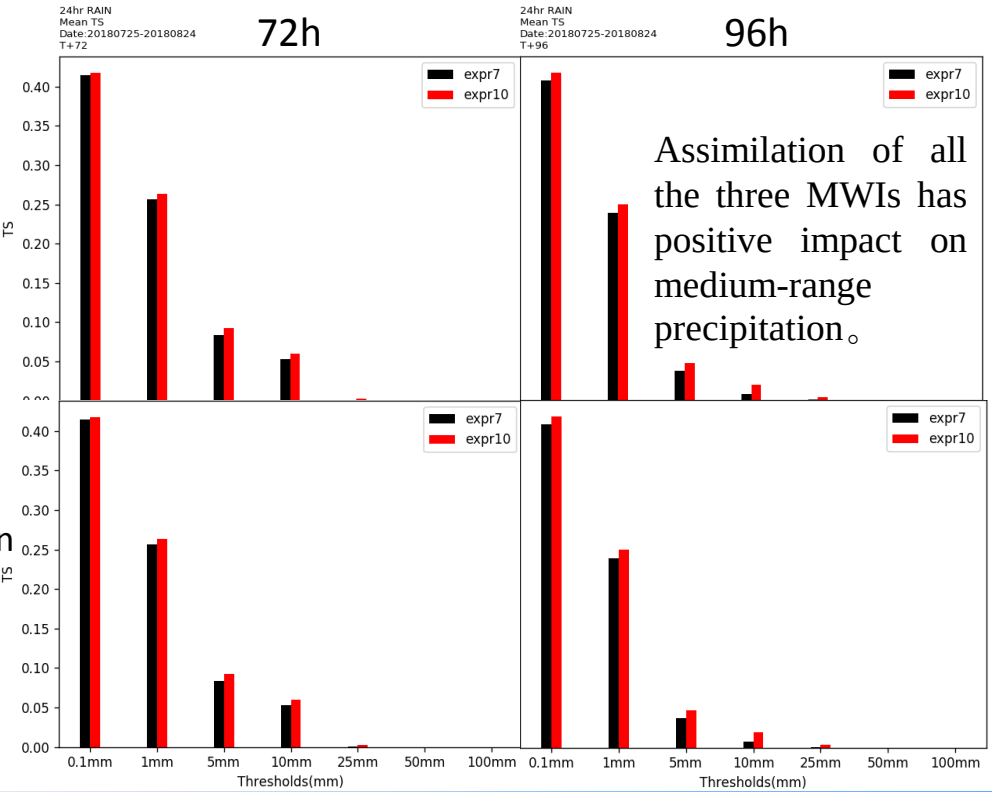

Assimilation of all the three MWIs has positive impact on medium-range precipitation。

Score Card for expr10 against expr7

Domain	Parameter	Level	Anomaly Correlation	RMS Error
NH	HGT	850		
		500		
		250		
	TEMP	850		
		500		
		250		
	UWND	850		
		500		
		250		
	VWND	850		
		500		
		250		
SH	HGT	850		
		500		
		250		
	TEMP	850		
		500		
		250		
	UWND	850		
		500		
		250		
	VWND	850		
		500		
		250		
EASI	HGT	850		
		500		
		250		
	TEMP	850		
		500		
		250		
	UWND	850		
		500		
		250		
	VWND	850		
		500		
		250		
TRO	HGT	850		
		500		
		250		
	TEMP	850		
		500		
		250		
	UWND	850		
		500		
		250		
	VWND	850		
		500		
		250		

▲: Far better ▲: Better : Better but not significant : Equality
▼: Far worse ▼: Worse : Worse but not significant

Assimilation of MWI: Future Plan

- The assimilation of MWIs' surface-sensitive channels over land;
- The assimilation of cloud and precipitation affected MWIs radiance.

Assimilation of MWI: Reference

Alishouse. J. C., S. Snyder, J. Vongsathorn, et al., 1990: Determination of oceanic total precipitable water from the SSM/I. IEEE Trans. Geosci. Remote Sens., 28, 811-816.

Bao, Y. S., F. Mao, J. Z. Min, et al., 2014: Retrieval of bare soil moisture from FY-3B/MWRI data. *Remote Sensing for Land and Resources*, **26**, 131-137.

Bouttier, F., and P. Courtier, 2002: Data assimilation concepts and methods march 1999. ECMWF.

Chen, H., and Y. Q. Jin, 2012: In-orbit intercalibration of FY-3B/MWRI and applications for monitoring drought and flooding. *J. Remote Sens.*, **16**, 1024-1034.

Chen, X. M., Q. J. Liu, and J. C. Zhang, 2007: A numerical simulation study on microphysical structure and cloud seeding in cloud system of QiLian Mountain Region. *Meteorological Monthly*, **33**, 33–43.

Dai, Y. J., X. B. Zeng, R. E. Dickinson, et al., 2003: The Common Land Model. *B. Am. Meteorol. Soc.*, **84**, 1013–1023.

Dou, F. L., D. W. An, and J. R. Li, 2014: Sea surface wind speed retrieval based on FY-3B Microwave Imager. *Remote Sensing Technology and Application*, **29**, 984-992.

Ferraro R. R., F. Z. Weng, N. C. Grody, et al., 1996: An eight-year (1987-1994) time series of rainfall, cloud, water wapor, snow cover, and sea ice derived from SSM/I measurements. *B. Am. Meteorolo. Soc.*, **77**, 891-905.

Geer, A. J., K. Lonitz, P. Weston, et al., 2018: All-sky satellite data assimilation at operational weather forecasting centres. *Q. J. R. Meteorol. Soc.*, **144**, 1191-1217.

Grody, N. C., and R. R. Ferraro, 1992: A comparison of passive microwave rainfall retrieval methods. Proceeding of the Sixth Conference on Meteorology and Oceanography. Washington, DC, American Meteorological Society, 60-65.

Han W. and N. Bormann, 2016: Constrained adaptive bias correction for satellite radiance assimilation in the ECMWF 4D-Var system, *ECMWF Tech. Mono*., **783**.

Harris, B. A., and G. Kelly, 2001: A satellite radiance-bias correction scheme for data assimilation. *Q. J. Roy. Meteorol. Soc.*, **127**, 1453-1468.

Hong, S. Y., and H. L. Pan, 1996: Nonlocal boundary layer vertical diffusion in a medium-range forecast model. *Mon. Wea. Rev.*, **124**, 2322–2339.

JAXA, 2013: GCOM-W1 SHIZUKU Data Users Handbook, Japan Aerospace Exploration Agency. Tsukuba, Japan. 125 pp. Available at http://gcom-w1.jaxa.jp/contents/GCOM-W1_SHIZUKU_Data_Users_Handbook_EN.pdf.

Kazumori, M., and Q. H. Liu, 2008: Impact study of AMSR-E radiances in the NCEP global data assimilation system. *Mon. Wea. Rev.*, **136**, 541-559.

Krasnopolsky, V. M., L. C. Breaker, and W. H. Gemmill, 1995: A neutral network as a nonlinear transfer function model for retrieving surface wind speeds from the special sensor microwave imager. *IEEE T. Geosci. Remote*, **100**, 11033-11045.

Lawrence, H., F. Carminati, W. Bell, et al., 2017: An evaluation of FY-3C MWRI and assessment of the long-term quality of FY-3C MWHS-2 at ECMWF and the Met Office, *ECMWF Tech. Mono*., **798**.

Li. L, E. Njoku, E. Im, et al., 2004: A preliminary survey of radio-frequency interference over the U.S. in Aqua AMSR-E data. *IEEE Trans. Geosci. Remote Sens.*, **42**, 380-390.

Liu, K., Q. Chen, and J. Sun, 2015: Modification of cumulus convection and planetary boundary layer schemes in the GRAPES global model. *J. Meteorol. Res.*, **29**, 806–822.

Liu, Z. Q., and F. Rabier, 2002: The interaction between model resolution, observation resolution and observation density in data assimilation: a one-dimensional study. *Q. J. Roy. Meteorol. Soc.*, **128**, 1367-1086.

Liu, Z. Q., C. S. Schwartz, C. Snyder, et al., 2012: Impact of assimilating AMSU-A radiances on forecasts of 2008 Atlantic tropical cyclones initialized with a limited-area Ensemble Kalman Filter. *Mon. Wea. Rev.*, **140**, 4017-4034.

Madrid, C., 1978: The Nimbus-7 User's Guide. NASA Goddard Space Flight Center.

Morcrette, J. -J., H. W. Barker, J. N. Cole, et al., 2008: Impact of a new radiation package, McRad, in the ECMWF integrated forecast system. *Mon. Wea. Rev.*, **136**, 4773-4798.

Oki, T., K. Imaoka, and M. Kachi, 2010: AMSR instruments on GCOM-W-1/2: concepts and applications//Proceedings of 2010 IEEE international Geoscience and Remote Sensing Symposium. Honolulu, HI: IEEE: 1363-1366.

Peng, L. C., W. B. Li, and H. Z. Liu, 2011: Estimation of the soil moisture using FY-3A/MWRI data over semiarid areas. *Acta Scientiarum Naturalium Universitatis Pekinensis*, **47**, 797-804.

Speen, G., L. Kaleschke, and G. Heygster, 2008: Sea ice remote sensing using AMSR-E 89-GHz channels. *J. Geophys. Res.: Oceans*, **113**, C02S03.

Sun, L. E., J. Wang, T. W. Cui, et al., 2012: Statistical retrieval algorithm of the sea surface temperature (SST) and wind speed (SSW) for FY-3B Microwave Radiometer Imager (MWRI). *J. Remote Sens.*, **16**, 1262-1271.

Tang, F., and X. L. Zou, 2017: Liquid water path retrieval using the lowest frequency channels of FengYun-3C microwave radiation imager (MWRI). *J. Meteor. Res.*, **31**, 1109–1122.

Tiedtke, M., 1993: Representation of clouds in large-scale models. *Mon. Wea. Rev.*, **121**, 3040–3061.

Weng, F. Z., N. C. Grody, R. Ferraro, et al., 1997: Cloud liquid water climatology from the special sensor microwave/imager. *J. Climate*, **10**, 1087-1098.

Wu, Y., and F. Z. Weng, 2011: Detection and correction of AMSR-E radio-frequency interference. *Acta Meteor. Sinica*, **25**, 669-681.

Xue, J. S., and D. H. Chen, 2008: *Scientific Design and Application of Numerical Prediction System GRAPES*. Beijing: Science Press, 383pp.

Yang, C., J. Z. Min, and Z. Q. Liu, 2017: The impact of AMSR2 radiance data assimilation on the analysis and forecast of Typhoon Son-Tinh. *Chinese J. Atmos. Sci.*, **41**, 372-384.

Yang, H., X. Q. Li, R. You, et al., 2013: Environmental data records from FengYun-3B Microwave Radiation Imager. *Advances in Meteor. Sci. Technol.*, **3**, 136-143.

Yu, Z. W., J. W. Liu, J. P. Huang, et al., 2017: Assimilation experiment of AMSR2 microwave imaging data and its influence on typhoon forecasting. *Meteorological, Hydrological and Marine Instruments*, **2**, 1-8.

Zhang, L., Y. Z. Liu, Y. Liu, et al., 2019: The operational global four-dimensional variational assimilation system at the China Meteorological Administration. *Q. J. R. Meteorol. Soc.*, **145**, 1882-1896.

Zhang, M., Q. F. Lu, S. Y. Gu, et al., 2019: Analysis and correction of the difference between the ascending and descending orbits of the FY-3C microwave imager. *J. Remote Sens.*, 23, 841-849.

Zhao, Y. L., 2012: Retrieval algorithm of sea surface wind vectors for WindSat based on a simple forward model. *Chin. J. Oceanol. and Limn.*, **31**, 210-218.

Zhou, Y. Q., and J. H. Yu, 2015: Circulation characteristics of track variation anomaly of tropical cyclone in the northwestern Pacific. *J. Meteorol. Sci.*, **35**: 720-727.

Zou, X. L., 2012: Introduction to microwave imager radiance observations from polar-orbiting meteorological satellites. *Adv. Meteor. Sci. Technol.*, **2**, 45-50.

Zou, X. L., J. Zhao, F. Z. Weng, et al., 2013a: Detection of radio-frequency interference signal over land from FY-3B Microwave Radiation Imager (MWRI). *IEEE Trans. Geosci. Remote Sens.*, **50**, 4994-5003.

END

Thank you for your attention!